Journal of Traditional and Complementary Medicine 14 (2024) 82–90

Contents lists available at ScienceDirect

Journal of Traditional and Complementary Medicine

journal homepage: http://www.elsevier.com/locate/jtcme

Gracilaria chorda subcritical-water extracts as ameliorant of insulin resistance induced by high-glucose in zebrafish and dexamethasone in L6 myotubes

Laxmi Sen Thakuri [a, b], Chul Min Park [c], Jin Woo Park [b, d], Dong Young Rhyu [a, b, *]

[a] Department of Nutraceutical Resources, Mokpo National University, Jeonnam, 58554, Republic of Korea
[b] Department of Biomedicine, Health & Life Convergence Sciences, BK21 FOUR, Mokpo National University, Jeonnam, 58554, Republic of Korea
[c] Inhalation Toxicity Research Group, Korea Institute of Toxicology, Jeongeup-si, Jeonbuk, 56212, Republic of Korea
[d] Department of Pharmacy, Mokpo National University, Jeonnam, 58554, Republic of Korea

ARTICLE INFO

Article history:
Received 29 December 2022
Received in revised form
8 July 2023
Accepted 18 July 2023
Available online 18 July 2023

Keywords:
Gracilaria chorda
Insulin resistance
L6 myotubes
Subcritical-water extract
Zebrafish larvae

ABSTRACT

Background and aim: Insulin resistance (IR) is a pathological condition in which cells fail to respond normally to insulin. Loss of insulin sensitivity disrupts glucose homeostasis and elevates the risk of developing the metabolic syndrome that includes Type 2 diabetes. This study assesses the effect on subcritical-water extract of *Gracilaria chorda* (GC) at 210 °C (GCSW210) in IR induction models of high glucose (HG)-induced zebrafish larvae and dexamethasone (DEX)-induced L6 myotubes.
Experimental procedure: The dose of HG and DEX for IR induction in zebrafish larvae and L6 myotubes was 130 mM or 0.5 μM. The capacity of glucose uptake was quantified by fluorescence staining or intensity. In addition, the activation of protein and mRNA expressions for insulin signaling (insulin-dependent or independent pathways) was measured.
Results and conclusion: Exposure of zebrafish larvae to HG significantly reduced the intracellular glucose uptake with dose-dependnet manner compared to control. However, the group treated with GCSW210 significantly averted HG levels like the insulin-treated group, and significantly up- or down-regulated the mRNA expressions related to insulin production (*insα*) and insulin signaling pathways. Moreover, the treatment with GCSW210 effectively regulated the protein expression of PI3K/AKT, AMPK, and GLUT4 involved in the action of insulin in IR models of L6 myotubes compared to DEX-treated control. Our data indicate that GCSW210 stimulates activation of PI3K/AKT and AMPK pathways to attenuate the development of IR induced by HG in zebrafish and DEX in L6 myotubes. In conclusion, GCSW210 is a potential agent for alleviating various diseases associated with the insulin resistance.

1. Introduction

Insulin resistance (IR) is clinically defined as the pathological conditions wherein cells lose sensitivity to the hormone insulin, resulting in reduced glucose uptake and utilization.[1] It is an attribute of obesity and type 2 diabetes mellitus (T2DM).[2] In T2DM, IR of the specific tissues increases the metabolic demand for insulin and eventually leads to the development of hyperglycemia. The pancreas copes with this by producing additional amounts of insulin, but this overproduction of insulin can eventually become futile, which results in impaired glucose transport.[3] Skeletal muscles are major target tissues of insulin and account for approximately 80% of the postprandial glucose intake and consumption caused by insulin stimulaiton.[4] However, when blood glucose levels are higher due to IR, skeletal muscles cannot respond to insulin appropriately because of severe damage to the insulin-stimulated glucose disposal mechanism; this leads to a defect in the insulin signaling pathway, a key feature of T2DM.[5] Therefore, increasing

* Corresponding author. Department of Nutraceutical Resources, College of Natural Sciences, Mokpo National University, 1666, Yeongsan-ro, Muan-gun, Jeonnam, 58554, Republic of Korea.
E-mail addresses: laxsen981@gmail.com (L.S. Thakuri), chulmin.park@kitox.re.kr (C.M. Park), jwpark@mokpo.ac.kr (J.W. Park), rhyudy@mokpo.ac.kr, rhyudy69@gmail.com (D.Y. Rhyu).
Peer review under responsibility of The Center for Food and Biomolecules, National Taiwan University.

https://doi.org/10.1016/j.jtcme.2023.07.006

Abbreviations

2-NDBG	2-[N-(7-nitrobenz-2-oxa-1,3-diazol-4-yl) amino]-2-deoxyglucose
AKT	protein kinase B
AMPK	AMP-activated protein kinase
CCK-8	cell counting kit 8
DMEM	Dulbecco's modified Eagle's medium
DEX	dexamethasone
FBS	fetal bovine serum
GC	*Gracilaria chorda*
GLUT-4	glucose transporter type 4
HG	high glucose diet
IR	insulin resistance
IRS-1	insulin receptor substrate-1
PBS	phosphate-buffered saline
PI3K	Phosphoinositide 3-kinase
PTEN	Phosphatase and tensin homolog
PVDF	polyvinylidene
qRT-PCR	real time quantitative reverse transcription -polymerase chain reaction
SW	subcritical water
SWE	subcritical water extract
T2D	type 2 diabetes
WST	water soluble tetrazolium salts

glucose uptake of skeletal muscles is an effective strategy to prevent diabetes.

The insulin signaling pathway is triggered when insulin connects with the membrane receptor of target cells, activating the phosphorylation of insulin receptor substrate-1 (IRS-1) that activates the phosphorylation of phosphoinositide 3-kinase (PI3K) and protein kinase B (AKT), which further activate the translocation of glucose transporter type 4 (GLUT4) from cytosol to cell-membrane. GLUT4 is the critical protein that control glucose uptake.[6] Therefore, the insulin-dependent PI3K/AKT signaling pathway is the primary molecular target for the treatment of IR.[7,8] Besides, AMP-activated protein kinase (AMPK) plays an important role in promoting glucose uptake in an insulin-independent manner.[9] Studies have reported that enhancement of AMPK signaling and its phosphorylation elevate GLUT4 expression, which essentially augments glucose uptake in various cell types.[10–12] As AMPK is an important cellular regulator of glucose metabolism, it has been considered a potential therapeutic target to ameliorate IR in treatment of T2DM.

Gracilaria chorda (GC) Holmes, also known as *Gracilariopsis chorda*, is a Rhodophyta belonging to the family Gracilariaceae and is known for its extensive medicinal benefits. Several studies have reported anti-oxidant, anti-bacterial, and anti-inflammatory effects of Gracilariaceae.[13,14] In previous study, we found that GCSW210 effectively regulates lipid accumulation and obesity-induced inflammation in 3T3L1 adipocytes or coculture system with macrophages. GCSW210 also significantly escalated glucose metabolism in co-cultures of adipocytes and RAW264.7 macrophages with or without insulin (100 nM). This result suggests that GCSW210 is a functional material with anti-diabetic and anti-obesity effects. However, an appropriate study on GCSW210 improving insulin resistance (IR) in type 2 diabetes models is necessary. So, the purpose of this study is to investigate anti-diabetic activities as obesity and obesity-induced inflammatory cytokines are mainly responsible for abnormalities in glucose metabolism and the induction of insulin resistance. Also, to study the characteristics mechanisms by which GCSW210 regulates glucose metabolism in IR models involving high glucose (HG)-induced zebrafish and dexamethasone (DEX)-induced L6 myotubes; dexamethasone and high glucose diet were chosen to induce IR *in vitro* and *in vivo*, respectively.

2. Materials and methods

2.1. Reagents

Cell Counting Kit-8 (Dojindo Laboratory, Kumamoto, Japan), dexamethasone (DEX), 3-isobutyl-1-methylxanthine (IBMX), insulin (IN) and Oil Red O were purchased from Sigma (St Louis, MO, USA). 2-[N-(7-nitrobenz-2-oxa-1,3-diazol-4-yl) amino]-2-deoxyglucose (2-NBDG) was purchased from Invitrogen (CA, USA). Beta-actin (sc-47778), GLUT4 (sc-53566) primary antibody and secondary antibody (anti-rabbit, anti-mouse) were purchased from Santa Cruz Biotechnology (Dallas, TX, USA) and p-IRS1 Ser307 (#2381), IRS1 (#2382), p-PI3K (#4228), PI3K (#4292), p-AKT (#9271), p-phosphatase and tensin homolog (p-PTEN, #9551), PTEN (#9559), AKT (#9272), p-AMPK (#2535), AMPK (#2532) primary antibodies were purchased from Cell Signaling Technology (Danvers, MA, USA). Polyvinylidene (PVDF) membrane was purchased from Bio-rad (Seoul, Korea), and all reagents used were high grade or first grade. Western blot chemiluminescent substrate and enzyme-linked immunosorbent assay kits SuperSignal™ West Pico PLUS Chemiluminescent Substrate, Mem-PER™ Plus Membrane Protein Extraction Kit (89842) were purchased from ThermoFisher (Seoul, Korea) and AsanPharm (Seoul, Korea), respectively.

2.2. Preparation of sample extracts

The preparation of GC extract was the same as that previously described.[15] Briefly, the crude extract was produced using subcritical water extractions process (TPR-1, TAIATSU TECHNO, Osaka, Japan) at 210 °C where 20g of GC was macerated in 200 mL of 3X distilled water; the reaction temperature for hydrolysis was maintained under a reaction pressure of 3 MPa for 1 min. Then the extracts were filtered under vacuum and freeze-dried for up to 72 h to yield 2.3g of powder GCSW210 (11.5% yield).

2.3. Cell culture and differentiation

L6 skeletal muscle cells were obtained from the American Type Culture Collection (Manassas, VA, USA) and cultured in Dulbecco's modified Eagle's medium (DMEM) medium supplemented with 10% fetal bovine serum (FBS) at 37 °C under 5% CO_2. The medium was replaced every two days. When cell growth achieved 80–90% confluence, the cells were seeded onto culture plates. For the differentiate of the cells from myoblasts to myotubes, the L6 cell medium was switched to DMEM with 2% (v/v) horse serum (HS). The L6 myoblast were allowed seven days to be fully differentiated.

2.4. Induction of insulin resistance in L6 myoblast and determination of cell cytotoxicity

L6 myoblasts were seeded onto 96-well plates at a density of 0.5×10^4 cells/well and allowed to be fully differentiated into myotubes. The myotubes were treated with 0.5 μM DEX for 24 h and further treated for 24 h at 37 °C with 5% CO_2 with different concentration of GCSW210 (125 or 250) μg/mL. Cell cytotoxicity

was observed using water soluble tetrazolium salt (WST) assay where CCK-8 solution (1 mg/mL) was added to each well. After 2 h of incubation, the absorbance was measured at a wavelength of 450 nm.

2.5. Western blot analysis

Cell lysates containing 15-20 μg of protein were separated by 10% sodium dodecyl sulfate polyacrylamide gel electrophoresis. Then transferred to a polyvinylidene difluoride (PVDF) membrane in a western blot apparatus (Bio-Rad, Hercules, CA, USA). The PVDF membrane was blocked with 5% skim milk for 1 h, rinsed with Tris-buffered-saline with Tween-20 (1 mol/L Tris, 5 mol/L NaCl, and 0.1% Tween 20), and incubated overnight with primary antibodies of IRS-1 (1:1000), PI3K (1:1000), PTEN (1:1000), AKT (1:1000), GLUT4 (1:250) and AMPK (1:1000). The PVDF membrane was then washed again with Tris-buffered-saline with 0.5% Tween-20, followed by incubation with secondary antibody (horseradish peroxidase-conjugated IgG 1:1000) for 1 h. Finally, the expressed proteins were quantified by analyzing the signals captured on a membrane using chemiluminescent substrate and Vision Works TMLS (Analysis software, Upland, CA, USA). To study the translocation of GLUT-4 proteins, cytosolic and membrane associated proteins were extracted following the provided manual of Mem-PER™ Plus Membrane Protein Extraction Kit (89842).

2.6. Zebrafish husbandry and toxicity assay

Wild-type adult zebrafish (*Danio rerio*, AB line) were cultured within a 14 h light/10 h dark cycle at a temperature of 28 °C with a pH of 7.0 in a flow-through system (Zebtec, Techniplast, Italy). All studies were carried out in accordance with the laboratory animal care standards established by the Mokpo National University and the American Veterinary Medical Association. Varying sizes of Gemma Micro Feed (Skretting Zebrafish; Tooele, UT, USA) were supplied to the zebrafish according to their developmental stage, twice or thrice a day. Adult male and female zebrafish were placed in mating tanks in the ratio 1:1, and the embryos were collected the next day. The healthy embryos were cultured in a 96-well plate with E2 embryo medium until 6 days-post-fertilization (dpf). At 6 dpf, the zebrafish larvae were treated with different concentrations of GCSW210 (125 and 250 μg/mL) and incubated for 24 h; Under an LEICA MZ10F microscope (Leica, Germany), the larvae were examined for viability and morphological abnormalities by comparing the relative size and shape of their eyes, yolk sacs, jaws, and tails to those of the normal group. The observed deformities and mortality rates were then evaluated.

2.7. Feeding protocol for zebrafish larvae in insulin resistance model

Larvae at 4dpf were divided into several groups (n = 40), with larvae intended to receive HG reared in glucose solutions (Sigma-Aldrich, CAS 50-99-7, G7021, St. Louis, MO, USA) of different concentration (32, 65, 130 mM), prepared in E2 medium (15 mM NaCl, 0.5 mM KCl, 1 mM $CaCl_2$, 1 mM $MgSO_4$, 0.150 mM KH_2PO4, 0.050 mM Na_2HPO_4, and 0.7 mM $NaHCO_3$, pH 7.1–7.4). Zebrafish larvae were exposed to D-glucose solution from 5 dpf to 8 dpf to induce insulin resistance.

2.8. Glucose uptake on zebrafish

To measure glucose uptake, the protocol laid down by Park et al.[16] was followed with some modification. Briefly, the seeded zebrafish larvae were first stained with 100 μL of 2-NBDG (600 μmol/L) and incubated for 3 h in the dark. Then, the zebrafish larvae were washed three times with E2 medium. Larvae from each group were anaesthetized with MS-222 (Tricaine, CAS: 888-86-2, Sigma-Aldrich, St. Louis, MO, USA). The fluorescence intensity of the zebrafish larvae was quantified using the ImageJ program (National Institutes of Health; Bethesda, MD, USA). Images of larvae were taken at 2.0 X and 4.0 X magnification using a LEICA MZ10F microscope with a mounted camera and iSolution software.

2.9. Quantitative reverse transcription-polymerase chain reaction

Total RNA was extracted from a pool of 40 larvae homogenized larvae using the Bullet blender homogenizer, and isolation was performed using the TRIzol reagent (Molecular Research Center, OH, USA). RNA primers were purchased from Integrated DNA Technologies (IA, USA). The quantitative RT-PCR (qRT-PCR) assays were conducted with the Applied Biosystems StepOne™ Real-Time PCR System Thermal Cycling Block (ABI, USA) using the SYBR Green Real-Time qPCR Kit (BIOFACT™, Daejeon, South Korea). The sequence of the oligonucleotide primers was preproinsulin (*insa*) –Forward: 5′- GGTGCTCTGTTGGTCCTGTT -3′ and Reverse: 5′-GGAGGAAGGAAACCCAGAAG -3′; insulin receptor substrate (*irs-1*) -Forward: 5′- AGGGTCTGGGTCACACAAAG -3′ and Reverse: 5′-GATCGGCCGACTTCAATAAA -3′; protein kinase (*akt*) -Forward: 5′-TCGGCAGGTGTCTTCTCAAT -3′ and Reverse: 5′ ACCCATTGCCA-TACCACGAG-3′; and AMP protein kinase (*ampk*) -Forward: 5′-AGTTATCAGCACACCGACAG -3′ and Reverse: 5′ AGTAATCCACCCCT-GAGATG -3′; qPCR reaction conditions were: 15 min at 95 °C, followed by 40 cycles of 15 s at 95 °C, 45 s at 60 °C, and plate analysis. Both positive and negative controls were included in each run. The number of gene copies was calculated by Ct value and standard curve. Significance analysis was performed on the log2 transformed values that were obtained via ANOVA analysis.

2.10. Statistical analysis

All statistical analyses were performed by one-way ANOVA and Dunnett's test using GraphPad Prism v5.03 (GraphPad Software, Inc., San Diego, CA USA). The data are expressed as the mean ± standard error of the mean (SE). Significant differences were defined for p-values of less than 0.05.

3. Results

3.1. Effect of GCSW210 on glucose uptake in zebrafish larvae

Zebrafish larvae did not exhibit any signs of toxicity including malformations until the concentration of GCSW210 reached 250 μg/mL (Fig. 1A). The survival rate was 100% (n = 12) in larvae treated with different concentrations of GCSW210 (Fig. 1B). As seen in Fig. 1C and D, both the intensity of image fluorescence and glucose uptake for the zebrafish larvae are observed to significantly increase when treated with GCSW210 in a dose-dependent manner compared to that in the control group.

3.2. Effect of high glucose exposure on glucose uptake in zebrafish larvae

Zebrafish larvae at 4 dpf were divided into several groups (n = 30) and exposed to HG at different concentrations (32, 65, and 130 mM). When zebrafish larvae were exposed to 65 and 130 mM of HG, the survival rate was reduced by approximately 20% and 22% compared to that in control group (Fig. 2A). Also, the exposure to HG resulted in decreased levels of image fluorescence and glucose uptake, with the amount of decrease depending on the concentration of the glucose solution (Fig. 2B and C). In the group exposed

A)

Indication of toxicity in zebrafish	Concentration (μg/mL)		
	0	125	250
No. of dead/ No. of total (embryos)	0/12	0/12	0/12
No. of malformed/ No. of survival (embryos)	0/12	0/12	0/12
Mortality (%)	100	100	100
Malformation (%)	0	0	0

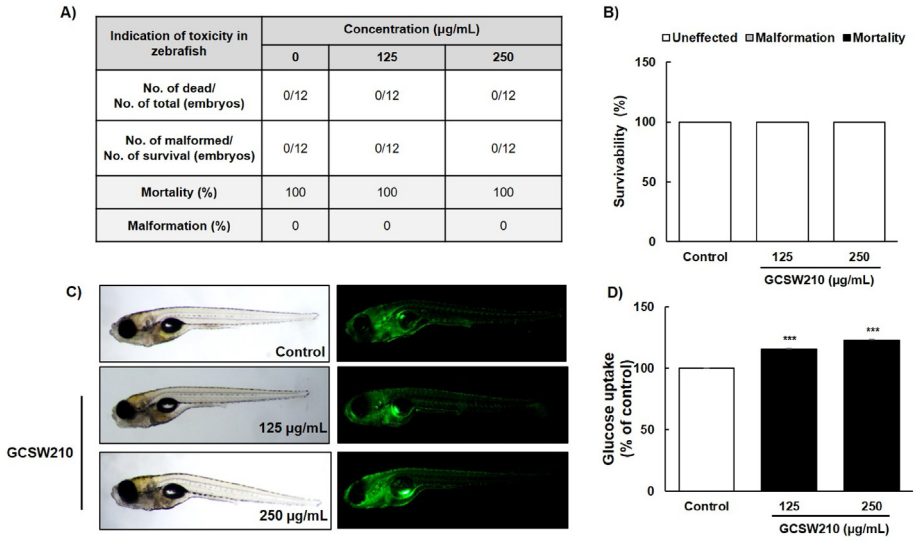

Fig. 1. Effect of GCSW210 on toxicity in and glucose uptake of zebrafish larvae. A) Indications of toxicity; B) survivability; C) fluorescence imaging of glucose uptake; D) level of glucose uptake. Fertilized eggs were collected and placed in 96-well culture plates. After 7 days post-fertilization (dpf), larvae were treated with GCSW210 (125 and 250 μg/mL) for 24 h post-fertilization (hpf), and mortality and malformation were observed. All values are presented as mean ± SE from three independent repeated experiments and analyzed by one-way analysis of variance followed by Dunnett test. *$p < 0.05$, **$p < 0.01$, ***$p < 0.001$ vs. control. Abbreviations: GCSW210; subcritical-water extract of Gracilaria chorda (GC) at 210 °C, dpf; days post-fertilization, hpf; hours post-fertilization.

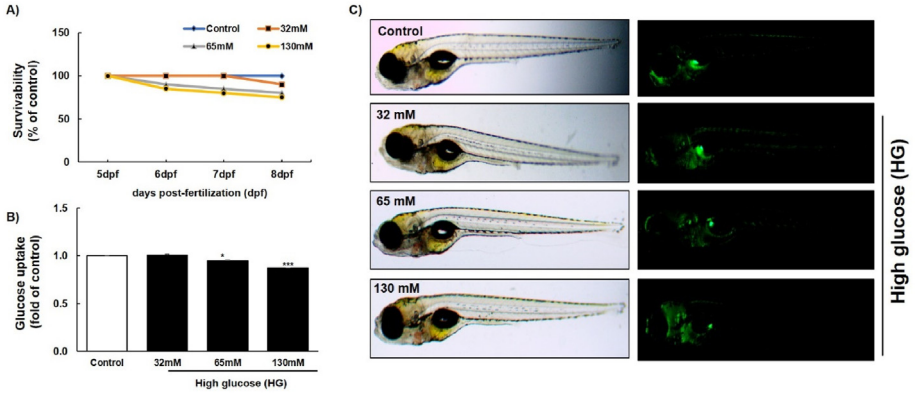

Fig. 2. Effect of HG on toxicity and glucose uptake of zebrafish larvae. A) survivability in different concentrations of glucose solution for 72 h; B) level of glucose uptake; C) fluorescence imaging of glucose uptake (2.0X). Zebrafish larvae were exposed to D-glucose solution (32, 65, and 130 mM) from 5 dpf to 8 dpf to induce IR to create a T2DM model. Data are presented as mean ± SE (n = 8) and analyzed by one-way analysis of variance followed by Dunnett test. *$p < 0.05$, **$p < 0.01$, ***$p < 0.001$ vs. control. Abbreviations: HG; high glucose, T2DM; type 2 diabetes mellitus.

to 130 mM glucose, the glucose uptake showed a significant reduction of 14% compared to that in the control group, indicating the induction of IR in zebrafish larvae (Fig. 2B).

3.3. Improvement following treatment with GCSW210 in insulin sensitivity of zebrafish larvae with insulin resistance

We evaluated glucose uptake and blood glucose levels after treatment with 100 nM insulin to confirm that IR induction or impairment of sensitivity was present in zebrafish larvae exposed to HG. Larvae exposed to HG showed significant reduction in glucose uptake of approximately 88%, and highly raised blood glucose levels of up to 148% compared to that in the control (Fig. 3). Also, the morphology of endocrine pancreas showed remarkable change after exposure to HG. This implies that the loss of insulin sensitivity is clearly associated with IR resulting from exposure to HG. Nevertheless, the increased blood glucose levels were effectively lowered by treatment with insulin or GCSW210, with greater reduction observed in the GCSW210-treated group. Our results reveal that GCSW210 improves glucose metabolism via increasing insulin sensitivity and pancreatic volume in HG-induced IR zebrafish larvae.

3.4. Upregulation following treatment with GCSW210 of insulin secretion and signaling pathway gene expressions in zebrafish larvae

The small body size of zebrafish larvae makes it impossible to isolate the mRNA of specific tissues without noticeable contaminations from surrounding tissues.[17] Therefore, we used real-time qPCR to examine the corresponding gene expression in the mRNAs extracted from the whole body homogenized lysate. The mRNA expression of *insa*, a human insulin precursor, was significantly enhanced to two-fold by exposure to HG, indicating an increase in metabolic demand due to hyperglycemia (Fig. 4A). Also, the mRNA expression of insulin-dependent signaling pathway

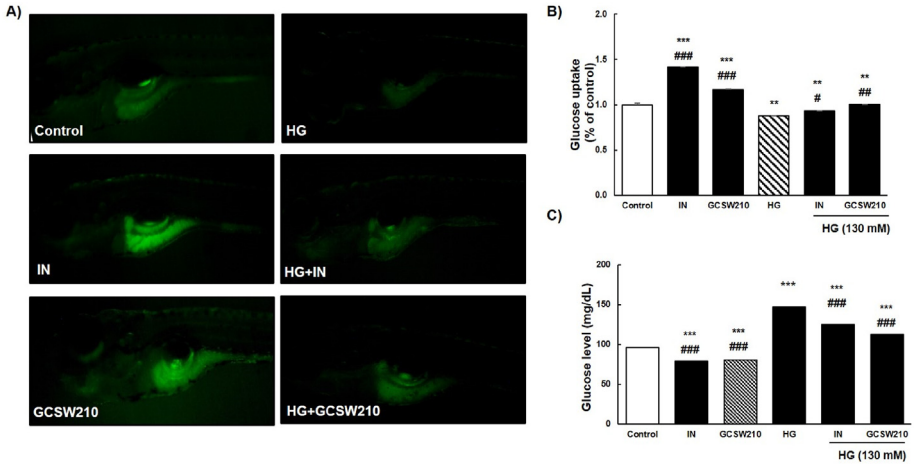

Fig. 3. Effect of GCSW210 on insulin sensitivity in HG-mediated insulin resistance model of zebrafish larvae. A) fluorescence imaging of glucose uptake (4.0X); B) level of glucose uptake; C) glucose level. Zebrafish larvae were exposed to D-glucose solution (130 mM) for 72 h starting 5 dpf to induce IR, followed by treatment with GCSW210 (250 μg/mL) for 24 h before determining glucose uptake. IN 100 nM was used as positive control. Data are presented as mean ± SE (n = 8) and analyzed by one-way analysis of variance. $^{*}p < 0.05$, $^{**}p < 0.01$, $^{***}p < 0.001$ vs control; $^{\#}p < 0.05$, $^{\#\#}p < 0.01$, $^{\#\#\#}p < 0.001$ vs high glucose (HG) group. Abbreviations: IN; insulin, IR; insulin resistance.

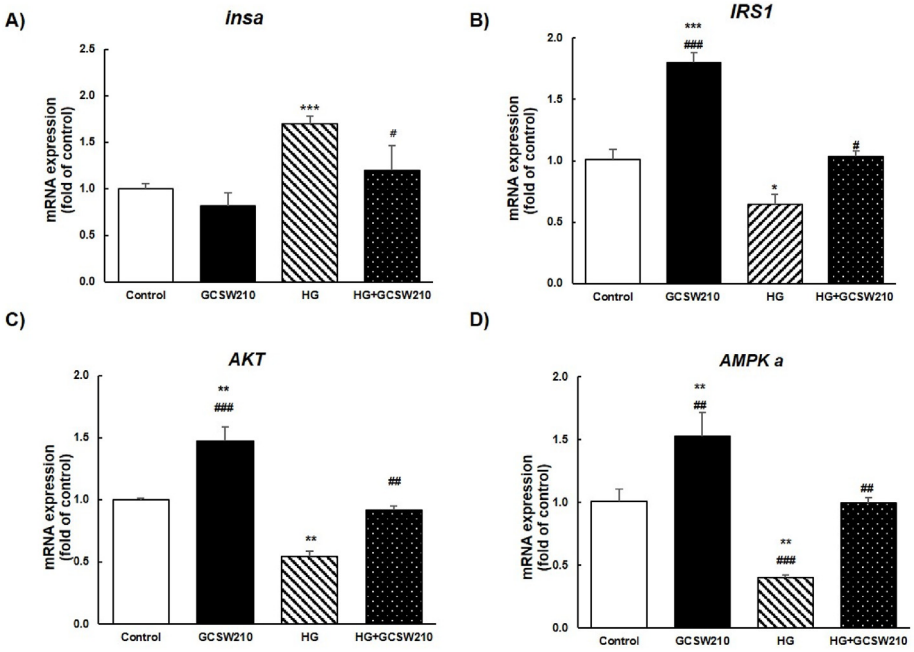

Fig. 4. Effect of GCSW210 on gene expressions in HG-mediated insulin resistance model of zebrafish larvae. A) *insa*; B) *irs1*; C) *akt*; D) *ampka*. Zebrafish larvae were exposed to D-glucose solution (130 mM) for 72 h starting 5 dpf to induce IR, followed by treatment with GCSW210 (250 μg/mL) for 24 h and homogenization. Data are presented as mean ± SE (n = 3) and analyzed by one-way analysis of variance. $^{*}p < 0.05$, $^{**}p < 0.01$, $^{***}p < 0.001$ versus control; $^{\#}p < 0.05$, $^{\#\#}p < 0.01$, $^{\#\#\#}p < 0.001$ versus HG. Abbreviations: GC; subcritical-water extract of *Gracilaria chorda* at 210 °C (GCSW210), HG; High glucose.

genes like *irs1* and *akt* was significantly decreased by 40% and 50%, respectively, in larvae with HG-induced IR compared to larvae in control group (Fig. 4B and C). AMPK mRNA expression was greatly suppressed to 40% in group exposed to HG (Fig. 4D). However, GCSW210 treatment in zebrafish larvae effectively increased the activation of mRNA genes closely associated with glucose metabolism in tissues under condition of hyperglycemia.

3.5. Improved glucose uptake in DEX-mediated IR L6 myotubes following treatment with GCSW210

The L6 myotubes differentiated from myoblasts were induced with IR when exposed to DEX at different concentrations (0.25–0.75 μM). DEX concentration of 0.5 and 0.75 μM produced cytotoxicity of approximately 15 and 30%, respectively, while compared to the control, groups treated with DEX at all concentration showed significantly reduced glucose uptake capacity (Fig. 5A and B). Based on these results, we used 0.5 μM DEX to promote insulin resistance in L6 myotubes. As shown in Fig. 5D, compared to the untreated normal group, DEX-treated group showed a significant 62% decrease in glucose uptake. GCSW210 naturally restored glucose uptake in DEX-mediated IR model of L6 myotubes, in a dose-dependent manner (Fig. 5D). The *in vivo* results being similar, GCSW210 can be considered a potential agent for improving IR.

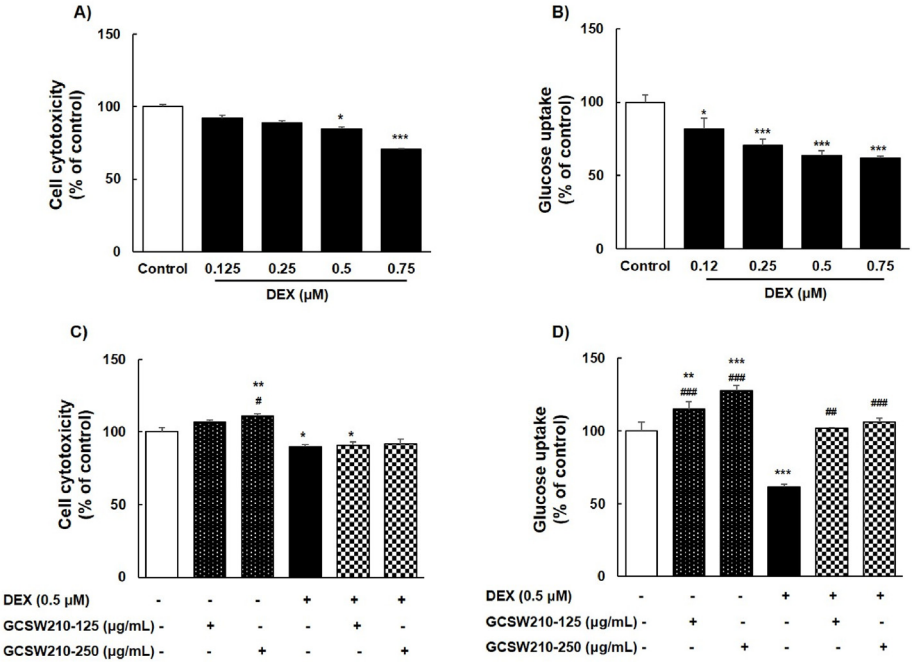

Fig. 5. Effect of GCSW210 on cell cytotoxicity and glucose uptake in DEX-mediated insulin resistance model of L6 myotubes. A) cytotoxicity produced by DEX; B) glucose uptake measured at various concentrations of DEX; C) cytotoxicity after GCSW210 treatment in DEX-mediated IR model; D) glucose uptake after GCSW210 treatment in DEX-mediated IR model. L6 cells were induced to differentiate with 2% HS and treated as indicated. After 24 h of treatment with 0.5 μM of DEX, L6 myotubes were further treated with 125 or 250 μg/mL of GCSW210, or with no GCSW210 added, for 24 h. Cell viability was determined using WST assay at 450 nm and glucose uptake was measured using 2-NDBG. Data are presented as mean ± SE (n = 6) and analyzed by one-way analysis of variance followed by Dunnett test. $^{*}p < 0.05$, $^{**}p < 0.01$, $^{***}p < 0.001$ vs. control; $^{\#}p < 0.05$, $^{\#\#}p < 0.01$, $^{\#\#\#}p < 0.001$ vs. DEX. Abbreviations: DEX; dexamethasone, HS; horse serum, 2-NBDG; 2-[N-(7-nitrobenz-2-oxa-1,3-diazol-4-yl) amino]-2-deoxyglucose.

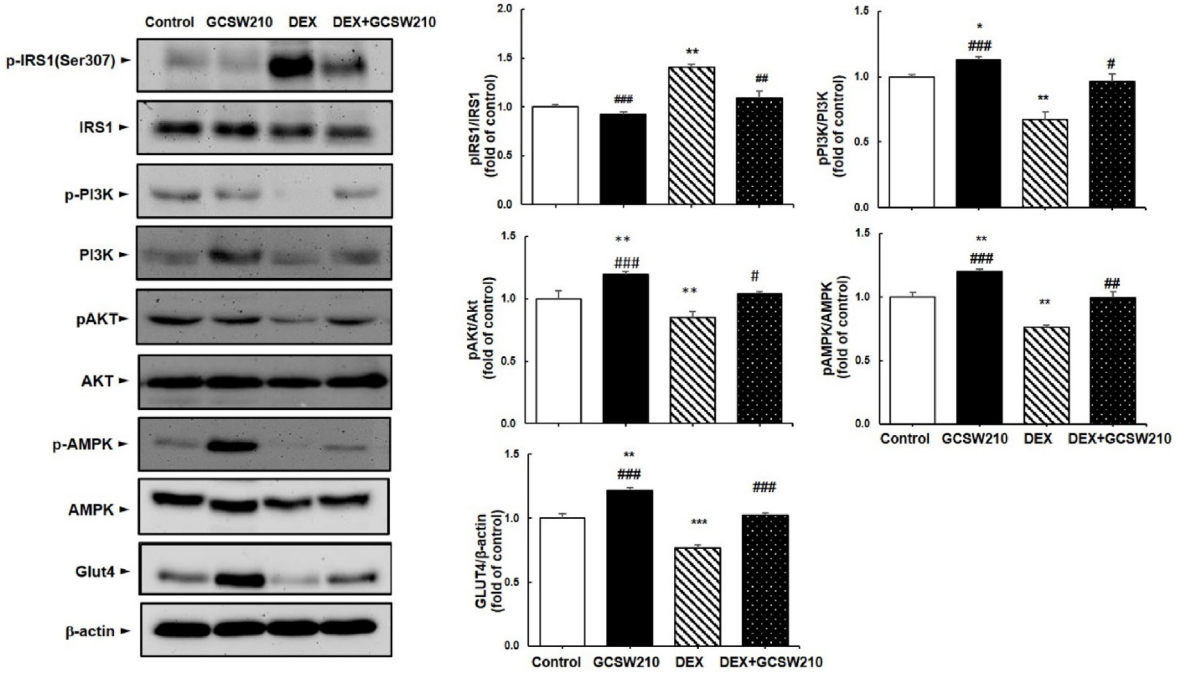

Fig. 6. Effect of GCSW210 on to glucose metabolism-related protein expression in DEX-indused insulin resistance model of L6 myotubes. L6 myoblast were induced to differentiate with 2% HS and treated as indicated. After 24 h of treatment with 0.5 mM of DEX, L6 myotubes were further treated with 250 μg/mL of GCSW210 or with no GCSW210, for 24 h. Data are presented as mean ± SE (n = 3) and analyzed by one-way analysis of variance followed by Dunnett test. $^{*}p < 0.05$, $^{**}p < 0.01$, $^{***}p < 0.001$ vs. control; $^{\#}p < 0.05$, $^{\#\#}p < 0.01$, $^{\#\#\#}p < 0.001$ vs. DEX. Abbreviations: DEX; dexamethasone, GC; subcritical-water extract of *Gracilaria chorda* at 210 °C (GCSW210).

3.6. Upregulation of protein expression related to glucose metabolism in DEX-mediated IR L6 myotubes following treatment with GCSW210

As evident from Fig. 6, the elevated expression of IRS-1 Ser307 phosphorylation that resulted from DEX stimulation was significantly reduced by GCSW210 treatment. In DEX-mediated IR model, the protein expressions of both the insulin-dependent PI3K/AKT and AMPK pathways were significantly inhibited, which in turn impacted GLUT4 glucose transport negatively (Fig. 7). However, treatment with GCSW210 significantly recovered the protein expression associated with glucose metabolism to near-normal levels. Moreover, PTEN is associated with IR as a negative regulator of dephosphorylated phosphatidylinositol-3,4,5-triphosphate (PIP3), which inhibits Akt activation.[18–20] As expected, a significant increase in PTEN levels was detected in DEX-induced group (approximately 34% compared to the control group). However, the level of p-PTEN in GCSW210 group was significantly lower than that in DEX group, indicating that GCSW210 significantly reversed these changes in PTEN expression (Fig. 8).

4. Discussion

In this study, we demonstrated the hypoglycemic effect of GCSW210 that influences glucose homeostasis in IR induced models of zebrafish larvae and L6 myotubes. We found that IR induced through exposure to DEX and HG effectively suppressed the expressions of proteins and genes related to insulin signaling and AMPK pathways, which eventually decreased glucose uptake in both models. However, the abnormal glucose metabolism following IR induction was remarkably reversed by GCSW210 treatment in both models. Thus, our results indicate that GCSW210 may prevent several chronic diseases like T2DM resulting from IR.

Zebrafish larvae were used as an *in vivo* insulin resistance model, as it has become an attractive model for studying human diseases due to their physiology being similar to that of mammals[21]; approximately 80% of all human disease genes have functional homologs in zebrafish.[22] Several studies have reported that the immersion of zebrafish in glucose solution (0.7–25%) results in diabetic complications that share similarities with complication in mice of streptozotocin-induced diabetes.[23,24] Also, Connaughton et al. (2016) reported that zebrafish immersed in glucose of 1% concentration showed high blood glucose levels that were significantly above control values.[25] Herein, we found that compared to the control group, zebrafish larvae exposed to a glucose solution of 130 mM (approximately 23%) exhibited the typical characteristics of IR such as low glucose uptake (about 12%) and high blood glucose level (approximately 48%). It is also significant that zebrafish have two preproinsulin genes, *insα* and *insβ*, of which *insα* is a prominent gene responsible for maintaining glucose homeostasis.[26,27] The group exposed to HG displayed upregulation of *insα* mRNA expression, which is involved in the compensatory response to hyperglycemia. Therefore, this model can induce not only hyperglycemia, but also insulin resistance.

Under normal conditions, insulin binds to the insulin receptor distributed on the cell membrane of target tissues, activating IRS. The activation of IRS plays a pivotal role in the functioning of insulin signaling transduction pathways such as the PI3K/AKT. Thus, the downregulation of the IRS leads to reduced insulin sensitivity and failure of the glucose metabolism.[28] Herein, zebrafish larvae exposed to HG exhibited downregulation of IRS1 and AKT mRNA expressions that promote glucose uptake. These triggered abnormalities as compared to the control group were significantly reversed by treatment with GCSW210 (250 μg/mL). We further confirmed the role of GCSW210 in this reversal using an *in vitro* model that used DEX to induce IR in L6 myotubes. Previous studies have reported that glucocorticoid inhibit glucose consumption by increased serine phosphorylation of IRS1 at residue 307.[29] In this study, we found that exposure to DEX produced a significant elevation in serine phosphorylation of IRS1 in L6 myotubes as well as a significant downregulation of phosphorylation of PI3K/AKT, in agreement with the findings of previous studies[30,31], resulting decreased GLUT4 expression and reduced glucose uptake. Likewise, PTEN is identified as a negative regulator of PI3K/AKT signaling as well as reported to impaired insulin signaling and promote insulin resistance.[32] In glucosamine-induced insulin-resistant skeletal muscle cells, the rate of glucose uptake, as well as the expression and translocation of GLUT4, were decreased, while the expressions of p-PTEN were elevated which suggestes that the increased PTEN expression is associated with the development of insulin resistance.[18] Song et al. (2020) also reported that PTEN inhibitor when used in diabetic mice, the protein expression of p-PI3K and p-AKT were higher.[32] In accordance to the previous findings, the results of the present study suggested that the increased expression of PTEN

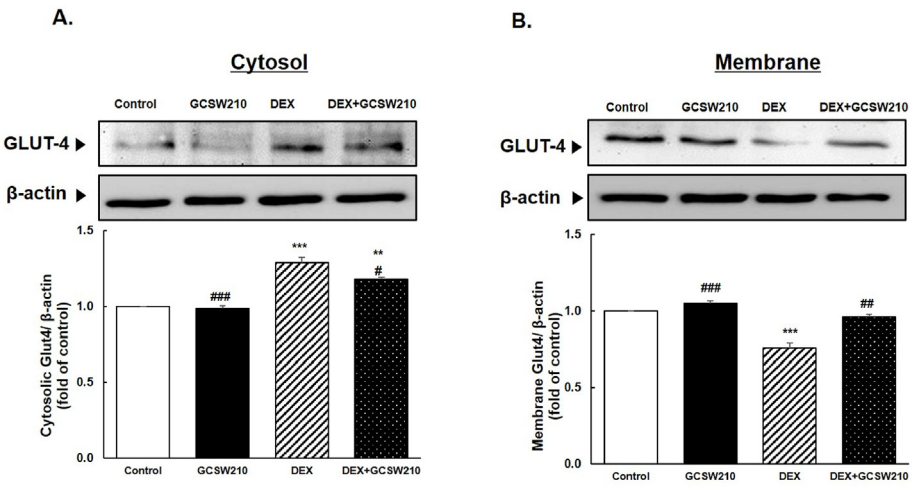

Fig. 7. Effect of GCSW210 on translocation of glucose transporters in DEX-induced insulin resistance model of L6 myotubes. A) cytosolic protein; B) membrane protein. Data are presented as mean ± SE (n = 3) and analyzed by one-way analysis of variance followed by Dunnett test. $^{*}p < 0.05$, $^{**}p < 0.01$, $^{***}p < 0.001$ vs. control; $^{\#}p < 0.05$, $^{\#\#}p < 0.01$, $^{\#\#\#}p < 0.001$ vs. DEX. Abbreviations: DEX; dexamethasone, GC; subcritical-water extract of *Gracilaria chorda* at 210 °C (GCSW210), GLUT4; Glucose transporter type 4.

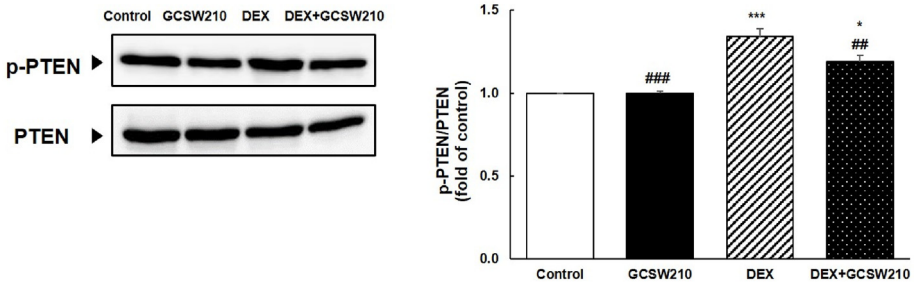

Fig. 8. Effect of GCSW210 on PTEN protein expression in DEX-induced insulin resistance model of L6 myotubes. Data are presented as mean ± SE (n = 3) and analyzed by one-way analysis of variance followed by Dunnett test. *$p < 0.05$, **$p < 0.01$, ***$p < 0.001$ vs. control; $^{\#}p < 0.05$, $^{\#\#}p < 0.01$, $^{\#\#\#}p < 0.001$ vs. DEX. Abbreviations: DEX; dexamethasone, GC; subcritical-water extract of *Gracilaria chorda* at 210 °C (GCSW210), PTEN; phosphatase and tensin homolog.

may induce a reduction in the translocation of GLUT4 in DEX-induced IR myotubes. However, the diabetogenic action of DEX was effectively attenuated by GCSW210 treatment. These results indicate that GCSW210 contributed significantly to increased glucose uptake by upregulating the insulin signaling cascades.

In addition to these insulin-dependent pathways, the activation of AMPK enhances activity of glucose transporter, GLUT4 in diverse cells and animal models.[33] AMPK is a master regulator that plays a role in cellular energy homeostasis and mediates glucose transportation.[34] Our results showed that GCSW210 treatment of zebrafish exposed to HG and L6 myotubes exposed to DEX effectively combats impairment of AMPK and GLUT4 expressions to increase glucose uptake. To the best of our knowledge, this discovery provides mechanistic insights into mechanism of protection against IR induced by DEX and HG in L6 myotubes and zebrafish larvae, respectively. Overall, our data suggest that GCSW210 facilitates glucose metabolism by combating IR via activating both PI3K/AKT insulin signaling and AMPK pathways.

5. Conclusion

Together, GCSW210 showed the potential to recover insulin signaling responses, presenting a new approach for the management of metabolic disorders. Further studies regarding the effect of GCSW210 are required to understand the mechanisms involved in maintaining glucose homeostasis, identifying the possible active compounds responsible for the anti-diabetic properties of GCSW210, thus providing an opportunity for the development of a new class of drugs.

CRediT authorship contribution statement

Laxmi Sen Thakuri: Formal analysis, Investigation, Writing-original draft preparation; Chul- Min Park: Investigation, Supervision, Writing-original draft preparation, Editing; Jin Woo Park: Funding acquisition, Editing; Dong-Young Rhyu: Conceptualization, Supervision, Funding acquisition, Methodology, Validation, Writing-review preparation, Editing.

Declaration of competing interest

The authors confirm that they have no conflict of interests with respect to the work described in this manuscript.

Acknowledgments

This research was supported by Basic Science Research Program through the National Research Foundation of Korea (NRF), funded by the Ministry of Education (2018R1D1A1B07050273), and by research funds from the Convergence Research Laboratory established by the Mokpo National University (MNU) Innovation Support Project in 2020. Also, this work was supported by the National Research Foundation of Korea (NRF) grant funded by the Korea government (MSIT) (No. 2022R1A5A8033794

References

1. Petersen MC, Shulman GI. Mechanisms of insulin action and insulin resistance. *Physiol Rev*. 2018;98(4):2133–2223. https://doi.org/10.1152/physrev.00063.2017.
2. Eckel RH, Grundy SM, Zimmet PZ. The metabolic syndrome. *Lancet*. 2005;365(9468):1415–1428. https://doi.org/10.1016/S0140-6736(05)66378-7, 2005/04/16/.
3. Stanford KI, Goodyear LJ. Exercise and type 2 diabetes: molecular mechanisms regulating glucose uptake in skeletal muscle. *Adv Physiol Educ*. 2014;38(4):308–314. https://doi.org/10.1152/advan.00080.2014, 2014/12/01.
4. He B, Shi M, Zhang L, et al. Beneficial effect of galanin on insulin sensitivity in muscle of type 2 diabetic rats. *Physiol Behav*. 2011;103(3):284–289. https://doi.org/10.1016/j.physbeh.2011.02.023, 2011/06/01/.
5. Tian C, Chang H, La X, Li J-a. *Wushenziye* formula improves skeletal muscle insulin resistance in type 2 diabetes mellitus via PTP1B-IRS1-Akt-GLUT4 signaling pathway. *Evid base Compl Alternative Med*. 2017:4393529. https://doi.org/10.1155/2017/4393529, 2017/12/31 2017.
6. Harriet Wallberg-Henriksson JRZ. GLUT4: a key player regulating glucose homeostasis? Insights from transgenic and knockout mice. *Mol Membr Biol*. 2001;18(3):205–211. https://doi.org/10.1080/09687680110072131, 2001/01/01.
7. Trevarrow B, Robison B. Genetic backgrounds, standard lines, and husbandry of zebrafish. *Methods Cell Biol*. 2004;77:599–616. https://doi.org/10.1016/S0091-679X(04)77032-6.
8. Abu Bakar MH, Cheng K-K, Sarmidi MR, Yaakob H, Huri HZ. Celastrol protects against antimycin A-induced insulin resistance in human skeletal muscle cells. *Molecules*. 2015;20(5):8242–8269. https://doi.org/10.3390/molecules20058242.
9. Kahn BB. Glucose transport: pivotal step in insulin action. *Diabetes*. 1996;45(11):1644–1654. https://doi.org/10.2337/diab.45.11.1644.
10. Shamshoum H, Vlavcheski F, MacPherson REK, Tsiani E. Rosemary extract activates AMPK, inhibits mTOR and attenuates the high glucose and high insulin-induced muscle cell insulin resistance. *Appl Physiol Nutr Metabol*. 2021;46(7):819–827. https://doi.org/10.1139/apnm-2020-0592, 2021/07/01.
11. Zhang Y, Zhu Z, Zhai W, Bi Y, Yin Y, Zhang W. Expression and purification of asprosin in Pichia pastoris and investigation of its increase glucose uptake activity in skeletal muscle through activation of AMPK. *Enzym Microb Technol*. 2021;144:109737. https://doi.org/10.1016/j.enzmictec.2020.109737, 2021/03/01/.
12. Entezari M, Hashemi D, Taheriazam A, et al. AMPK signaling in diabetes mellitus, insulin resistance and diabetic complications: a pre-clinical and clinical investigation. *Biomed Pharmacother*. 2022;146:112563. https://doi.org/10.1016/j.biopha.2021.112563, 2022/02/01/.
13. Kim H-M, Kang S-I, Shin H-S, et al. Anti-obesity effect of komulkosiraegi [Gracilaria vermiculophylla (Ohmi) Papenfuss] extract in 3T3-L1 cells. *Food Sci Biotechnol*. 2012;21(1):83–89. https://doi.org/10.1007/s10068-012-0010-8, 2012/02/01.
14. Mohibbullah M, Hannan MA, Choi J-Y, et al. The edible marine alga Gracilariopsis chorda alleviates hypoxia/reoxygenation-induced oxidative stress in cultured hippocampal neurons. *J Med Food*. 2015;18(9):960–971. https://doi.org/10.1089/jmf.2014.3369.
15. Thakuri LS, Park CM, Park Jin Woo, Kim HA, Rhyu DY. Subcritical water extraction of Gracilaria chorda abbreviates lipid accumulation and obesity-induced inflammation. *ALGAE*. 2023;38(1):81–92. https://doi.org/10.4490/algae.2023.38.12.26.

16. Park C-M, Kim K-T, Rhyu D-Y. Exposure to a low concentration of mixed organochlorine pesticides impairs glucose metabolism and mitochondrial function in L6 myotubes and zebrafish. *J Hazard Mater*. 2021;414:125437. https://doi.org/10.1016/j.jhazmat.2021.125437, 2021/07/15/.
17. Jung S-H, Kim YS, Lee Y-R, Kim JS. High glucose-induced changes in hyaloid-retinal vessels during early ocular development of zebrafish: a short-term animal model of diabetic retinopathy. *Br J Pharmacol*. 2016;173(1):15–26. https://doi.org/10.1111/bph.13279.
18. Wang DF, Yang HJ, Gu JQ, et al. Suppression of phosphatase and tensin homolog protects insulin-resistant cells from apoptosis. *Mol Med Rep*. 2015;12(2):2695–2700. https://doi.org/10.3892/mmr.2015.3771.
19. Xing Y, Zhang J, Wei H, et al. Reduction of the PI3K/Akt related signaling activities in skeletal muscle tissues involves insulin resistance in intrauterine growth restriction rats with catch-up growth. *PLoS One*. 2019;14(5):e0216665. https://doi.org/10.1371/journal.pone.0216665.
20. Bulger DA, Conley J, Conner SH, Majumdar G, Solomon SS. Role of PTEN in TNFα induced insulin resistance. *Biochem Biophys Res Commun*. 2015;461(3):533–536. https://doi.org/10.1016/j.bbrc.2015.04.063.
21. Gut P, Reischauer S, Stainier DYR, Arnaout R. Little fish, big data: zebrafish as a model for cardiovascular and metabolic disease. *Physiol Rev*. 2017;97(3):889–938. https://doi.org/10.1152/physrev.00038.2016.
22. Langheinrich U. Zebrafish: a new model on the pharmaceutical catwalk. *Bioessays*. 2003;25(9):904–912. https://doi.org/10.1002/bies.10326.
23. Gleeson M, Connaughton V, Arneson LS. Induction of hyperglycaemia in zebrafish (Danio rerio) leads to morphological changes in the retina. *Acta Diabetol*. 2007;44(3):157–163. https://doi.org/10.1007/s00592-007-0257-3, 2007/09/01.
24. Jörgens K, Hillebrands JL, Hammes HP, Kroll J. Zebrafish: a model for understanding diabetic complications. *Exp Clin Endocrinol Diabetes*. 2012;120(4):186–187. //23.04.2012.
25. Connaughton VP, Baker C, Fonde L, Gerardi E, Slack C. Alternate immersion in an external glucose solution differentially affects blood sugar values in older versus younger zebrafish adults. *Zebrafish*. 2016/04/01 2016;13(2):87–94. https://doi.org/10.1089/zeb.2015.1155.
26. Papasani MR, Robison BD, Hardy RW, Hill RA. Early developmental expression of two insulins in zebrafish (Danio rerio). *Physiol Genom*. 2006;27(1):79–85. https://doi.org/10.1152/physiolgenomics.00012.2006, 2006/09/01.
27. Michel M, Page-McCaw PS, Chen W, Cone RD. Leptin signaling regulates glucose homeostasis, but not adipostasis, in the zebrafish. *Proc Natl Acad Sci USA*. 2016;113(11):3084. https://doi.org/10.1073/pnas.1513212113.
28. Oliveira JM, Rebuffat SA, Gasa R, Gomis R. Targeting type 2 diabetes: lessons from a knockout model of insulin receptor substrate 2. *Can J Physiol Pharmacol*. 2014;92(8):613–620. https://doi.org/10.1139/cjpp-2014-0114, 2014/08/01.
29. Morgan SA, Sherlock M, Gathercole LL, et al. 11β-Hydroxysteroid Dehydrogenase Type 1 regulates Glucocorticoid-induced insulin resistance in Skeletal muscle. *Diabetes*. 2009;58(11):2506–2515. https://doi.org/10.2337/db09-0525.
30. Hasselgren P-O. Glucocorticoids and muscle catabolism. *Curr Opin Clin Nutr Metab Care*. 1999;2(3):201–205.
31. Stitt TN, Drujan D, Clarke BA, et al. The IGF-1/PI3K/Akt Pathway Prevents Expression of muscle atrophy-induced ubiquitin ligases by inhibiting FOXO transcription factors. *Mol Cell*. 2004;14(3):395–403. https://doi.org/10.1016/S1097-2765(04)00211-4, 2004/05/07/.
32. Song Y, Liu W, Tang K, Zang J, Li D, Gao H. Mangiferin alleviates renal interstitial fibrosis in streptozotocin-induced diabetic mice through regulating the PTEN/PI3K/Akt signaling pathway. *J Diabetes Res*. 2020;2020:9481720. https://doi.org/10.1155/2020/9481720.
33. Qiu J, Maekawa K, Kitamura Y, et al. Stimulation of glucose uptake by theasinensins through the AMP-activated protein kinase pathway in rat skeletal muscle cells. *Biochem Pharmacol*. 2014;87(2):344–351. https://doi.org/10.1016/j.bcp.2013.10.029, 2014/01/15/.
34. Hardie DG, Ross FA, Hawley SA. AMPK: a nutrient and energy sensor that maintains energy homeostasis. *Nat Rev Mol Cell Biol*. 2012;13(4):251–262. https://doi.org/10.1038/nrm3311, 2012/04/01.